Earth and Planetary Science Letters 369–370 (2013) 98–107

Contents lists available at SciVerse ScienceDirect

Earth and Planetary Science Letters

journal homepage: www.elsevier.com/locate/epsl

Tide-modulated gas emissions and tremors off SW Taiwan

Shu-Kun Hsu [a,*], Shiou-Ya Wang [a], Yen-Che Liao [a], Tsanyao F. Yang [b], Sen Jan [c], Jing-Yi Lin [a], Song-Chuen Chen [a,d]

[a] Department of Earth Sciences, National Central University, Taiwan
[b] Department of Geosciences, National Taiwan University, Taiwan
[c] Institute of Oceanography, National Taiwan University, Taiwan
[d] Central Geological Survey, Ministry of Economic Affairs, Taiwan

ARTICLE INFO

Article history:
Received 6 October 2012
Received in revised form
10 March 2013
Accepted 12 March 2013
Editor: P. Shearer
Available online 16 April 2013

Keywords:
tide
gas emission
tremor
mud volcano
Taiwan

ABSTRACT

The continental margin off SW Taiwan is in an incipient stage of orogeny and contains numerous active mud diapirs and mud volcanoes. Gas emissions out of the seabed off SW Taiwan are revealed by acoustic images from 38 kHz echo sounders or sub-bottom profilers. However, the mechanism for gas emissions is still poorly understood. In this study, we show that the gas emissions out of the seabed and the associated tremors off SW Taiwan are strongly correlated with the ocean tides, especially with the diurnal and semidiurnal constituents. Particularly, for each tidal day the strong gas emissions (expulsions) and long-duration tremors occur mainly during both the rising periods to the higher high tides and the falling periods to the lower low tides. Both the gas emissions and tremor activities are generally quiescent near the tidal datum. On average, the daily intensity of gas emissions and the magnitude of tremors are positively proportional to the daily tidal range; a larger slope site implies a greater concentration of gas in the shallow sediments. Most of the individual tremors and long-duration tremors observed off SW Taiwan occur as results of the strong gas expulsions out of the gas-bearing seabed. The high-frequency components of the induced tremors quickly decay and are followed by horizontal low-frequency (~7 Hz) harmonic oscillations of the seabed. Long-duration tremors may enhance seafloor instability and increase the potential for submarine landslides.

1. Introduction

In addition to the methane emissions from fossil fuel related anthropogenic sources, geologic emissions of methane also have great impacts on the geosphere, the biosphere, the hydrosphere and the atmosphere (Etiope and Klusman, 2002; Judd, 2003). Among all, methane escape from the seafloor is a widespread phenomenon (Judd, 2003). The out-going free methane out of seabed is mainly derived from the dissociation of gas hydrate, formed at a high pressure and low temperature environment (Sloan, 1998). The bottom of the gas hydrate stability zone below the seafloor is often marked by a BSR (Bottom Simulating Reflector) in reflection seismic profiles. Gas hydrate may dissociate when the seafloor becomes shallow. The result can induce an over-pressure pore-fluid in marine sediments. The fluid, mainly methane and carbon dioxide, may migrate upwards through gas seepage and produce mud volcanoes or pockmarks (Kopf, 2002; Judd and Hovland, 2007; Dimitrov, 2003).

The area off SW Taiwan is situated in the northern end of the Manila subduction zone. As shown in Fig. 1, the BSR is widely distributed off SW Taiwan (Chi et al., 2006; Liu et al., 2006) but there is almost no BSR at water depths less than ~600 m. It indicates that the gas hydrate in the area off SW Taiwan becomes unstable and disassociates at a water depth around 650 m. Free methane may be effectively produced in the area off SW Taiwan due to two main facts. First, the area is gradually uplifted and shoals due to a NW–SE plate convergence between the Philippine Sea Plate and the Eurasian Plate and an incipient stage of the Taiwan orogeny (e.g. Sibuet and Hsu, 2004; Lo and Hsu, 2005). Second, the global warming increases seafloor temperatures. Thus, gas-related mud diapirs and mud volcanoes are distributed from the offshore to the onshore area of SW Taiwan (Yang et al., 2004; You et al., 2004; Chiu et al., 2006) (Fig. 1). Moreover, high methane fluxes were detected in both cored sediments (Chuang et al., 2006, 2010; Lim et al., 2011) and water column samples (Yang et al., 2006). Among all the mud volcanoes, the submarine mud volcano MV1 is ~100 m high above a seafloor of ~450 m deep (Fig. 1). The MV1 is active as illustrated by its steep cone-shaped morphology and the flowing gas bubbles out of its summit into the seawater, which are detected as a gas plume by a 38 kHz echo sounder.

Active mud volcanoes cannot only emit methane but also generate micro-earthquakes or tremors (Judd and Hovland, 2007). To understand the mechanism of gas emission from the seabed and the tremors off SW Taiwan, we deployed 8 short-period OBSs

* Corresponding author. Tel.: +886 3 4268316; fax: +886 3 4222044.
E-mail address: hsu@ncu.edu.tw (S.-K. Hsu).

0012-821X/$ - see front matter © 2013 Elsevier B.V. All rights reserved.
http://dx.doi.org/10.1016/j.epsl.2013.03.013

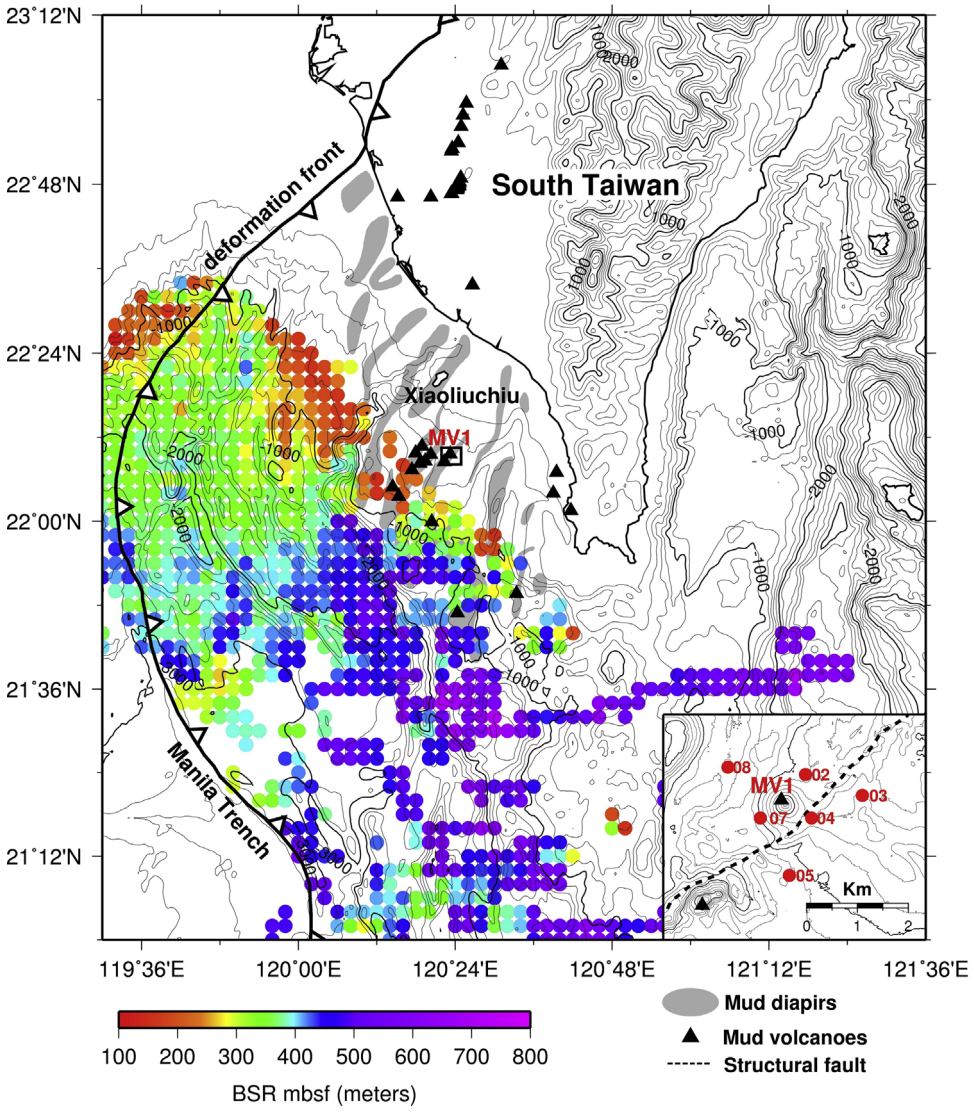

Fig. 1. Topography and structural features in northern Manila subduction zone (in southern Taiwan). A distribution of $2' \times 2'$ gridded BSR is plotted. The inset shows the locations of the active mud volcano MV1 and the locations of the deployed OBSs (in numbers). mbsf: meters below seafloor.

(Ocean Bottom Seismometer) around the MV1 from May 4 to May 25, 2011 (Fig. 1). However, one deployed OBS was lost and one had a recording malfunction. Each of the 6 remaining OBSs has recorded 3 components geophone and one hydrophone data for 22 days. We used air-gun shooting data to calibrate the OBS horizontal orientations.

2. Gas emissions

2.1. Emitting gases and modes

Active mud volcanoes in the area off SW Taiwan are intermittently emitting gases out of the seabed. To measure the gas contents of the seawater above MV1, the seawater column was sampled at 10 different depths in a 9-grid cell around MV1. As shown in Fig. 2a and b, MV1 emits high concentrations of CH_4 and CO_2 into the seawater. The high concentrations of CH_4 and CO_2 near seafloor suggest that they may derive from a deep source. Observed by a ROV camera near the seafloor, mudflows from the summit of MV1 can be observed. MV1 is sometimes quiescent but sometimes eruptive. During each eruption, MV1 discharges gases and debris into the seawater (Fig. 2c and d). Based on bathymetric or side-scan sonar images, we may also observe related pockmarks on the nearby seafloor (Chen et al., 2010), which also indicate gas expulsions out of the seafloor. On the other hand, deeper gases may also come to shallow strata in a much quieter way through gas seepage. Thus, unlike the seafloor morphology of mud volcanoes or pockmarks, those gas seeps can be observed as gas chimneys or vertically acoustic blanking columns in shallow seismic profiles or sub-bottom profilers. In consequence, the seafloor has gentle morphology. However, owing to persistent gas charging into shallow strata, some uppermost sedimentary layer may be arched due to a high-pore pressure. We may also discover some associated authigenic carbonates on the seafloor by detecting the strong backscatter images of sidescan sonar (Chen et al., 2010).

2.2. Temporal variation

To understand the activity of gas emissions out of MV1, we observed the gas plumes over the summit of MV1 by analyzing the acoustic images of the water column from a 38 kHz echo sounder. For that, we sailed back and forth over the MV1 for more than 24 h. The acoustic images over the summits of the mud volcano display a temporal variation of the gas emission activity (Fig. 3). In comparison

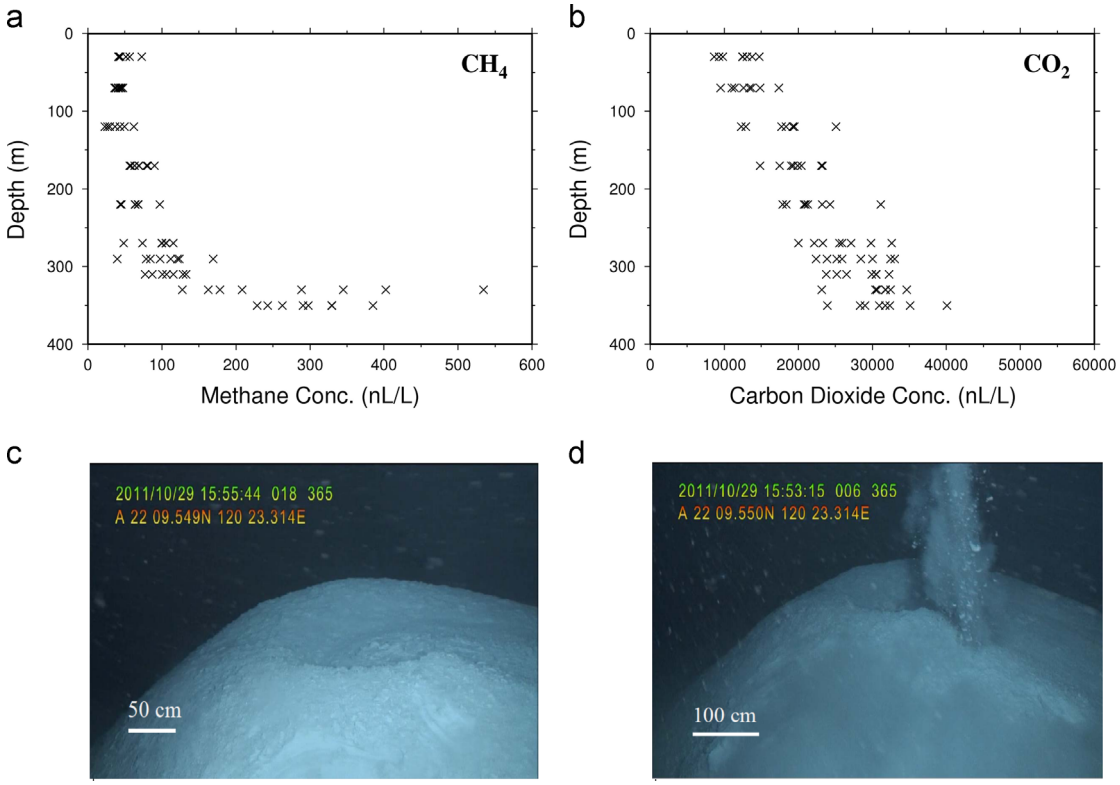

Fig. 2. The concentrations of emitting gases above the mud volcano MV1 and the ROV photos of MV1. (a) A vertical distribution of the CH_4 concentration. (b) A vertical distribution of the CO_2 concentration. (c) A MV1 photo during a gas-emission quiet period. (d) A MV1 photo during a strong gas expulsion period.

with the ocean tide from a nearby tide gauge (Xiaoliuchiu), the strongest activity of gas emission (or high concentration of CH_4 and CO_2) occurs during the rising period to the higher high tide (period A2) (Fig. 4). In contrast, the weakest activities occur during the periods near the tidal datum (periods A1, A5 and A7) or during the falling period to the tidal datum (period A3) (Fig. 4). The former could be related to very small stress rates from the tidal variation. The latter could be attributed to an insufficient recharge of free methane from a deeper source to shallow sedimentary layers in a short time immediately after the strong emission period of A2. The mechanism for the strong gas emission in period A6 could be also due to an increasing stress rate as in period A2; however, the stress rate and the gas emission are relatively smaller than in period A2 (Fig. 4). The A4 is at the falling period to the lower low tide. Its increasing gas emission could be due to a decreasing pressure on the seabed and an increasing methane supply from the methane hydrate dissociation.

3. Gas-induced tremors

3.1. Impulse tremors and long-duration tremors

In all the 6 OBSs data, at least 4 kinds of seismic signals can be recognized: (1) individual impulse tremors that occur sporadically over the time (Fig. 5); (2) as long as 6 h long-duration tremors (Fig. 5); (3) several plate interface earthquakes that can be identified by all the geophones; (4) very low-frequency earthquakes that can only be identified by the 6 hydrophones but not or not clearly by the geophones. Individual and long-duration tremors are both lack of coherency among all the OBSs; however, the occurrence of the long-duration tremors at each station shows a systematic delay (Fig. 5). In this study, we focus on the two kinds of tremors that are linked to the gas emissions out of the seabed. The lack of coherency for the tremors could be because each tremor source is too small and localized near only one OBS, not necessary from MV1. That could explain why each tremor source is rarely detected simultaneously by any two or more OBSs.

To understand the natures of the impulse or the long-duration tremors off SW Taiwan, we analyzed the particle motions of a paradigmatic tremor (Fig. 6a). The particle motion in the first period t1 in Fig. 6 indicates a high-frequency primary (P) wave with longitudinal motion along a NE–SW direction. In period t2, the particle motion contains both the longitudinal and transverse components and is ascribed to a secondary (S) wave. Immediately after, the particle motion is dominated by a ~7 Hz low-frequency oscillation as demonstrated in period t3. The damped harmonic motion follows the P-wave direction but without significant vertical components (Fig. 6b). This indicates that the tremor originates from a near-seafloor source linked to a sudden expulsion of the gas out of the seabed; the seafloor then oscillates at its natural frequency, around 7 Hz. In fact, it is often observed that only the portion of the harmonic motion of an individual tremor is recorded because the high-frequency portions quickly decay. During a long-duration tremor, the seabed also intensively oscillates at low frequency and the vertical component of the seabed oscillation is also relatively weak. A long-duration tremor is thus considered as the superposition of consecutive impulse tremors. The result is similar to many concurrent low-frequency earthquakes for a non-volcanic tremor in subduction zones (Shelly et al., 2006).

3.2. Correlation between tidal ranges and tremor amplitudes

To know the temporal variation of tremor activity at each OBS site, we calculated the amplitudes (envelopes) of seismic signals from the 3 components of the geophone data. For comparison, the tidal variation in the same period from the tide gauge of the

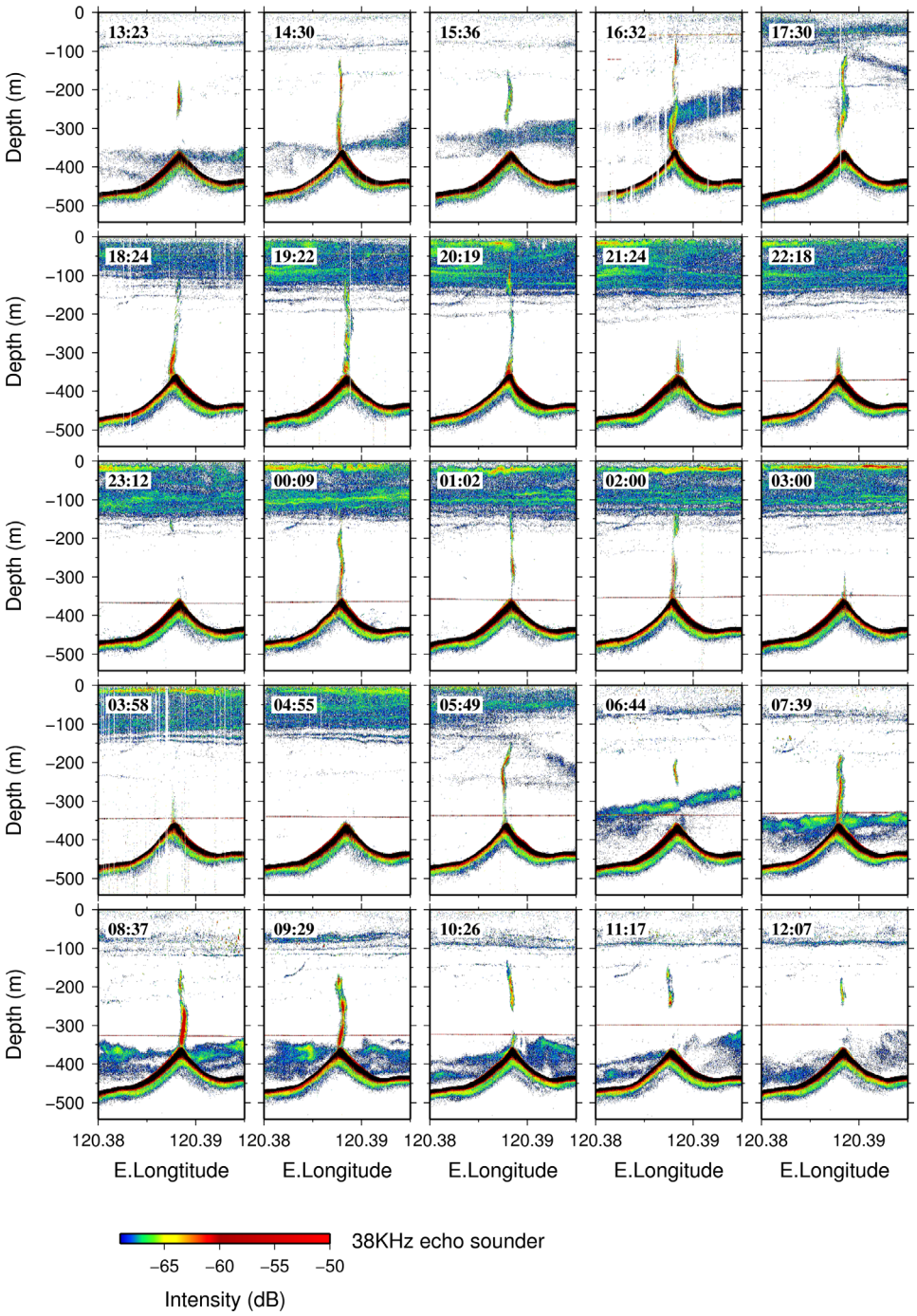

Fig. 3. The gas plume images of a 38 kHz echo sounder over the mud volcano MV1, which are collected over a span of 24 h on November 11, 2011. The time shown in the upper-left corner of each inset is the moment when the research vessel was passing over the summit of the mud volcano. It is noted that there is a temporal variation of the gas emission intensity.

Xiaoliuchiu islet was used (see location in Fig. 1). The tidal curve at Xiaoliuchiu is very similar to a simulated model at the location of MV1 (Hu et al., 2010). As the example from OBS05 (Fig. 7a), the tremor activity is larger near the spring tide and smaller near the neap tide. We calculated the average amplitude of the tremors over each tidal day and compared with its corresponding tidal range. We found that the tremor amplitude is in direct proportion to the tidal range at each OBS site (Fig. 7b). In other words, the tremor activity depends on the tidal change rate. It suggests that the tremor activity has a monthly variation due to the Moon's orbital motion around the Earth. Moreover, every OBS site has a different tremor amplitude response to the same tidal range. The larger gradients of the tremor amplitude relative to the tidal range exist at OBS03 and OBS05 sites (Fig. 7b), which is probably due to the existence of more compressible gases in the shallow sediments around OBS03 and OBS05 sites. However, the OBS03 and OBS05 sites are both situated in the right-hand side of a NE–SW trending fault located to the SE of MV1 (Fig. 1).

3.3. Correlation with ocean tides

Applying a power spectrum analysis for the time series of the tremor amplitudes, we find that the occurrence of the tremors is strongly related to the ocean tides. The tidal constituents of O_1, K_1,

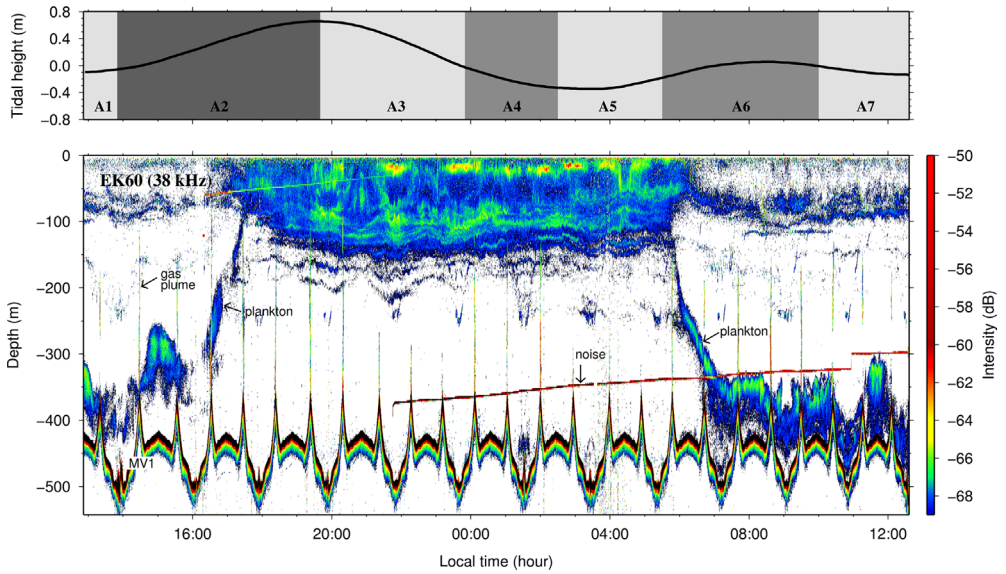

Fig. 4. A comparison between the tidal variation and the one-day acoustic image of a 38 kHz echo sounder across MV1 on November 11, 2011. The ship was sailing back and forth in a NE-SW direction. Note that the strongest gas emissions (plumes) in the water column occurred during the rising period to the higher high tide (the period of the dark gray area A2), while the weaker gas emissions occurred around the relatively flat tides (the periods of the light gray areas A1, A5 and A7) or after the higher high tide (the period of A3). The close-up images of the gas plumes are shown in Fig. 3.

M_2, K_2, M_3, MK_3, M_4, $2MK_5$ and M_6 are especially pronounced for the OBS03 and OBS05 data (Fig. 7c). The tidal modulation of the semidiurnal and diurnal constituents was found in non-volcanic tremors in subduction zones (Rubinstein et al., 2008; Nakata et al., 2008; Lambert et al., 2009), non-volcanic tremors in transform faults (Thomas et al., 2009), volcanic tremors (Custodio et al., 2003) or micro-seismicity in axial volcanoes of mid-ocean ridges (Tolstoy et al., 2002; Kasahara, 2002). However, the large amplitudes of the tremors in our study area do not only favor the occurrence at high waters (Shelly et al., 2007; Rubinstein et al., 2008) or at low waters (Tolstoy et al., 2002). By blowing up Fig. 7a for the period around the spring tide, our results indicate that the tremor activity is much more quiescent near the tidal datum (Fig. 8a and b). Most of the large and long-duration tremors tend to occur during both the rising periods to the higher high tides (light red areas in Fig. 8a) and the falling periods to the lower low tides (light blue areas in Fig. 8a). Especially, the largest tremors generally occur at high tides and largest positive stress rates, or at low tides and largest negative stress rates (Fig. 8a and b). Fig. 8c shows the correlation coefficient and phase difference diagrams from the cross-spectrum analysis between the time series of tremors and the tides at OBS03, OBS04 and OBS05 sites. It shows that the diurnal and semidiurnal tides dominate the tremor activity; however, the tremor amplitudes are positively correlated to the diurnal tides but inversely to the semidiurnal tides (Fig. 8c). That is, a group of long-duration tremors occurs around the crests of the diurnal tides (light red areas in Fig. 8a) and a group of long-duration tremors occurs around the troughs of the semidiurnal tides (light blue areas in Fig. 8a). In both groups, a split of the tremor activities could be observed in the crest of a diurnal tide or in the trough of a semidiurnal tide (Fig. 8a). The split is due to the slight difference between two close constitutes of the diurnal (O1 and K1) or the semidiurnal tides (M2 and K2) (Fig. 7c). This phenomenon is similar to the split of the peak values of gas flow observed in the near-shore area of Santa Barbara, California (Boles et al., 2001), where the increasing gas flow occurs at low tides.

It is noticed that the ocean tides only provide several kPa stress variation on the seabed but the correlation with constituent M_6 can even be detected in the tremor activity. It suggests that the high pore-fluid pressure within the seabed is near vertical stress and the gas-related tremor activity is very sensitive to a minor tidal or vertical stress change.

4. Discussion

Comparing the temporal distribution of the gas emission and the tremor activities, we can find that their strong activities occur in coincidence (cf. Figs. 4 and 8). The dominance of horizontal low-frequency oscillations in the seabed indicates that the tremors are caused by the strong gas expulsions (eruptions) out of the seabed.

The daily variation of the long-duration tremors and the methane emissions can be regarded as a tidal pumping effect. The tidal variation provides the vertical stress variation for the pore fluid beneath the overlying sediments. When the ocean tide wanes, the decreasing pressure induces the unstable methane hydrate to dissociate and cause more free methane to migrate upward. Free methane then accumulates beneath the temporarily dilating shallow strata and excessive methane is expelled out of the seabed. When the ocean tide rises, the increasing pressure inhibits deep gas hydrate dissociation but increases pore-fluid pressure in the shallow strata. The increasing pressure in the shallow strata also increases the methane concentration in pore water. When the pore-fluid pressure is greater than the “failure strength” of the overlying sediments, shallow gases are intensively expelled out of the seabed and consequently more tremors are created. Here the failure strength is considered as the summation of the vertical stress (from the overlying sediments and seawater) and the yield stress of the overlying sedimentary layer if the overlying sediments can deform plastically. However, in most of the cases, the pore-fluid pressure just needs to exceed the vertical stress because the gas emissions and tremors happen daily. Such an ocean tidal pumping effect consistently transforms the shallow methane hydrate to free methane gas, which is then transported into the seawater or even the atmosphere. Then again, the recharge of methane could be from the deeper free methane that migrates upwards along the bottom of the tilted methane hydrate layer.

During each tidal day, although large gas emissions and tremors are generally observed in both the rising periods to the higher high

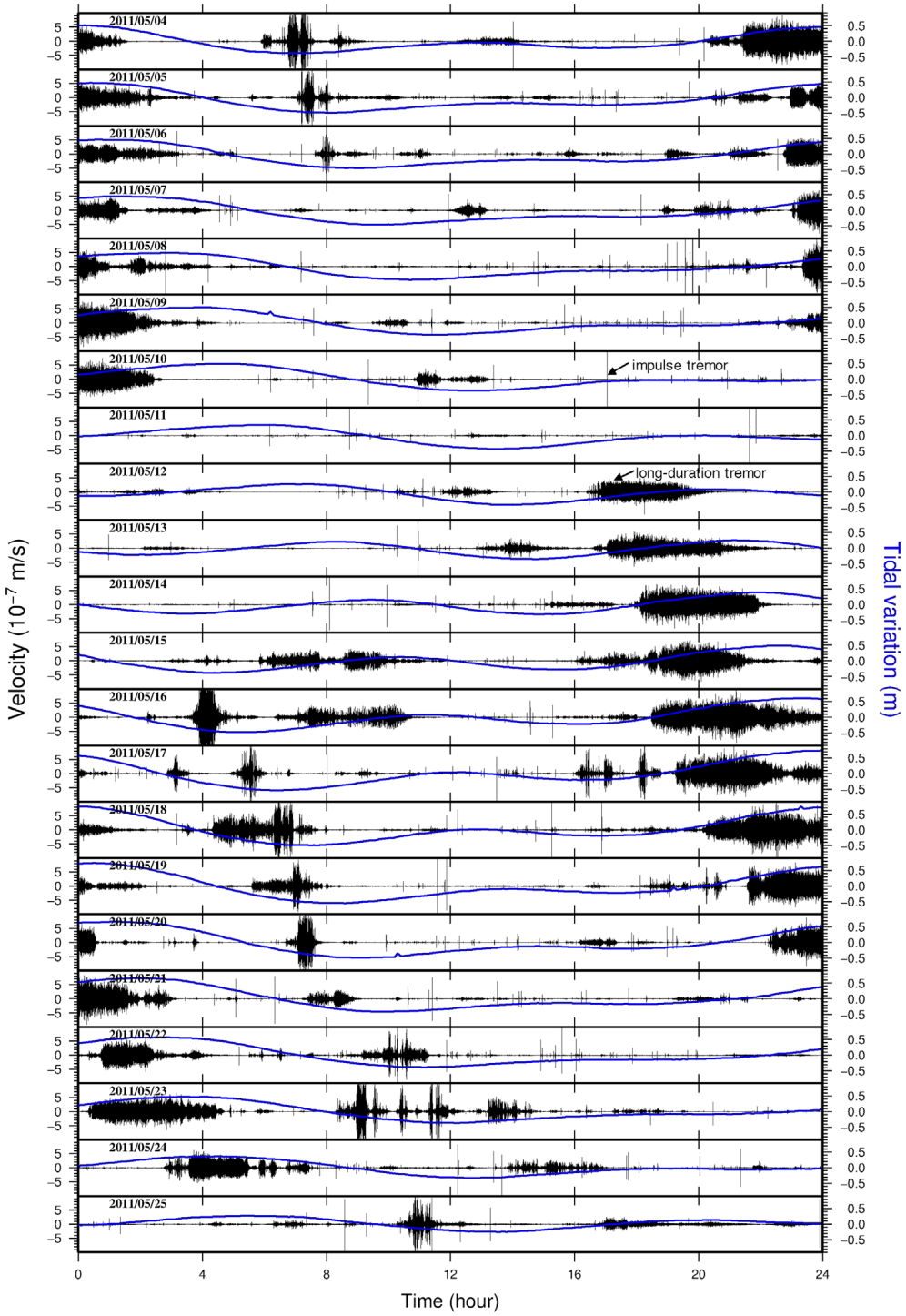

Fig. 5. Temporal variation of the vertical components of velocity amplitudes of OBS 5 for the whole recording period. It is noted that sporadically individual tremors and periodic long-duration tremors exist. The tidal variation (marked in blue) from a nearby tide gauge of Xiaoliuchiu islet is plotted for reference. (For interpretation of the references to color in this figure legend, the reader is referred to the web version of this article.)

tides and the falling periods to the lower low tides (Figs. 4 and 8), the strongest activity usually occur at the former ones. It is especially true for OBS03 and OBS05 sites whose response of the tremor amplitude to the tidal change is more obvious (Fig. 7b). However, for a weak response site such as OBS02 (Fig. 7b), especially during the period around the neap tide, the large and long-duration tremors usually occur at low waters (Fig. 9). The largest gas emission near each low tide may be explained by using a pore activation model (Boles et al., 2001). Nevertheless, the model fails to explain the largest gas emission at each rising period to the higher high tides. To understand the relationship between gas emissions, tremor activities and tides on the basis of our results, at least two factors are involved: first, the gas supply from deeper sources to the shallow strata, and second, the vertical stress of the overlying sediments. In the context of a sufficient gas supply such as at OBS03 or OBS05 site, the gas charge in the shallow sediments can cause over-pressure fluid overcoming the vertical stress of the overlying sediments in either the increasing stress field during rising tides or the decreasing stress field during the waning tides. However, for a fixed depth beneath the seabed, the vertical stress in

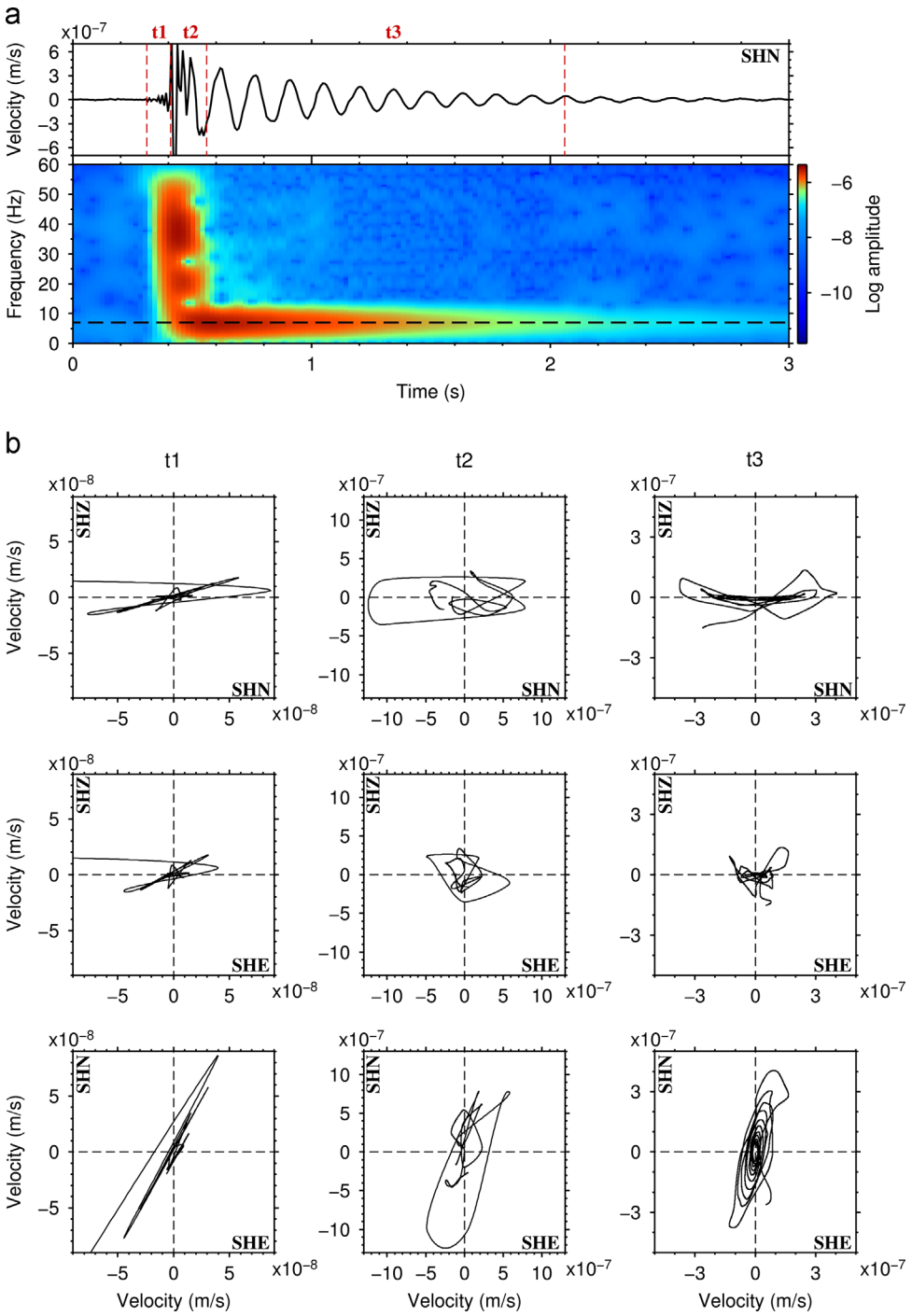

Fig. 6. Spectrum and particle motions of the N–S component of an individual tremor recorded by OBS 5 from 19:41:30 of May 5, 2011. (a) The window Fourier transform result of the tremor which contains the first arrival of a high-frequency P-wave (in period t1). The S-wave follows the P-wave (in period t2). Afterwards, the seabed oscillates horizontally at a low-frequency of ~7 Hz. (b) The particle motions at different periods of t1, t2 and t3. Note that the harmonic motion in period t3 is along with the P-wave propagation direction and there are no significant vertical-motions (SHZ).

a high tide is always greater than in a low tide. Thus, the gas expulsions and tremors are usually stronger in the rising periods to the higher high tides.

In the context of an insufficient gas supply such as at OBS02 site, the pore-fluid pressure due to less gas-charging rate from a low tide to a high tide may not overcome the vertical stress of the overlying sediments in the increasing stress field (rising tide), thus no violent gas expulsions and tremors. However, the pore pressure may still overcome the vertical stress of the overlying sediments in a decreasing stress field (waning tide). In some cases, it is also observed that the pore-fluid pressure may not overcome the vertical stress in the rising period to the higher high tides, but the continuously increasing pore-fluid pressure due to the gas charging finally results in the large gas emission in the period of the decreasing stress field after the higher high tide. It can be imagined that in the context of a very low gas-charging rate or the charging gas cannot be retained beneath shallow sedimentary strata (due to silent gas seeps through sandy layers or through crustal fissures or fractures), the overlying sedimentary strata are not broken in only one or few tidal cycles. After all, gas expulsions

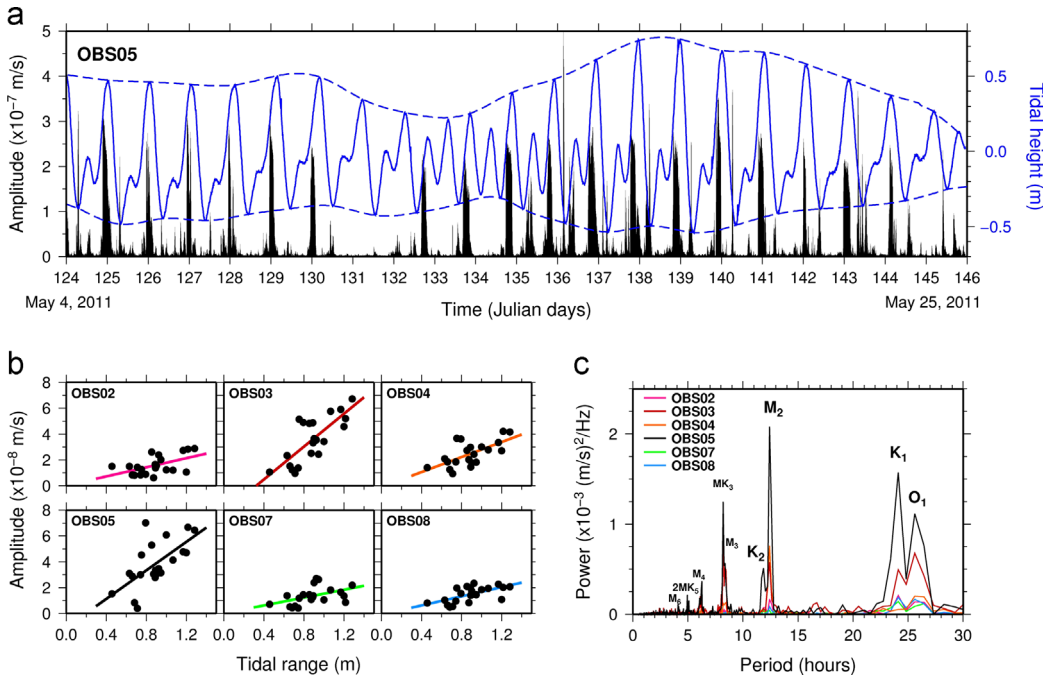

Fig. 7. Relationship between the tremors and the ocean tides. (a) The time series of velocity amplitudes summed every 6 min (in black) at OBS 5 and the corresponding tidal variation (in blue). Note that the amplitudes of the seismic tremors show a periodic variation and the maximum amplitudes usually appear at rising periods to higher high tides. (b) A linear relationship exists between the tremor amplitudes and the tidal ranges at each OBS site. The amplitude is the average of all the amplitudes in a tidal day. (c) The power spectrum density of the tremor amplitudes at each OBS site. Note that the tremor activity closely depends on the ocean tides, especially on the diurnal and semidiurnal constituents. (For interpretation of the references to color in this figure legend, the reader is referred to the web version of this article.)

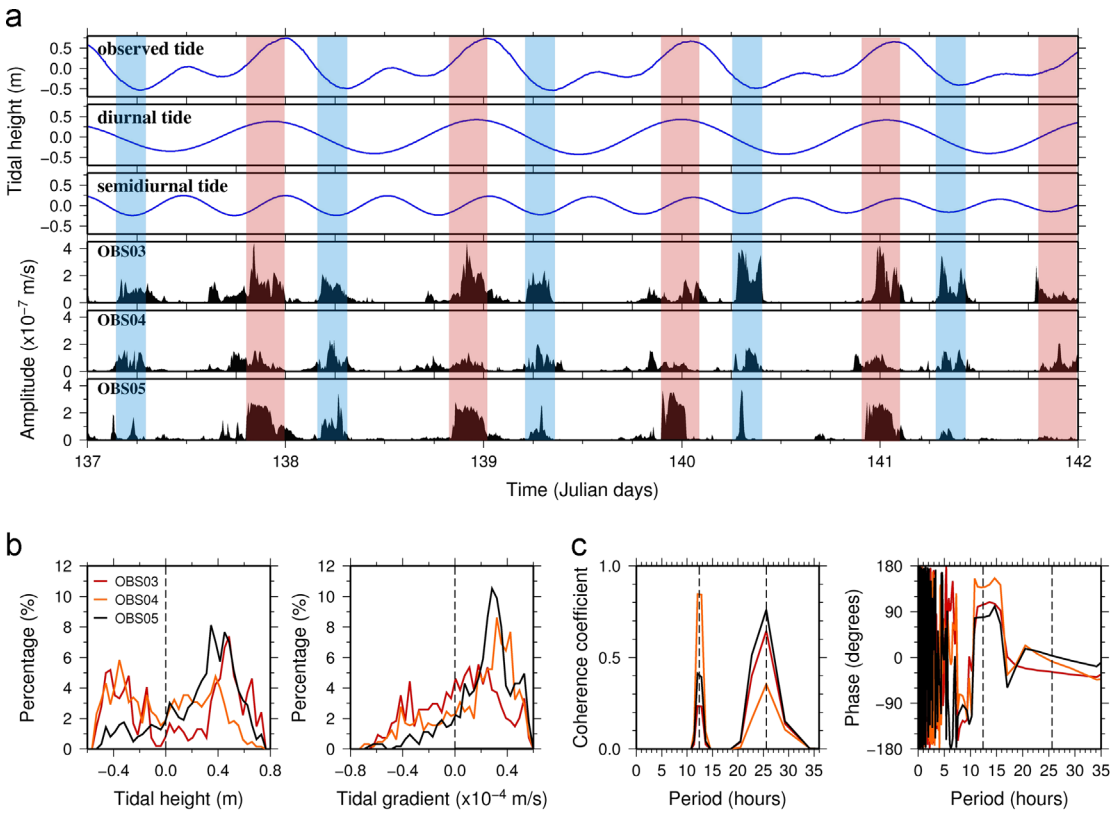

Fig. 8. (a) Close-ups of the tremor activities at OBS03, OBS04 and OBS05 sites, compared to the observed tides, diurnal and semidiurnal constituents, respectively, from May 17 to May 21, 2011. The light red areas mark the long-duration tremors occurring during the rising periods to the higher high tides. The light blue areas mark the long-duration tremors occurring during the falling periods to the lower low tides. (b) Statistics for the top 80% tremors amplitudes summed in every 6-min for the whole data recorded at OBS03, OBS04 and OBS05 sites. It is noted that the tremors are relatively quiet near the tidal datum. Largest tremors tend to occur at positive high waters and positively tidal slopes. (c) Cross-spectrum between the tremors and the tides. Note that the tremor activity is positively dependent on the diurnal constituents but inversely on the semidiurnal constituents. (For interpretation of the references to color in this figure legend, the reader is referred to the web version of this article.)

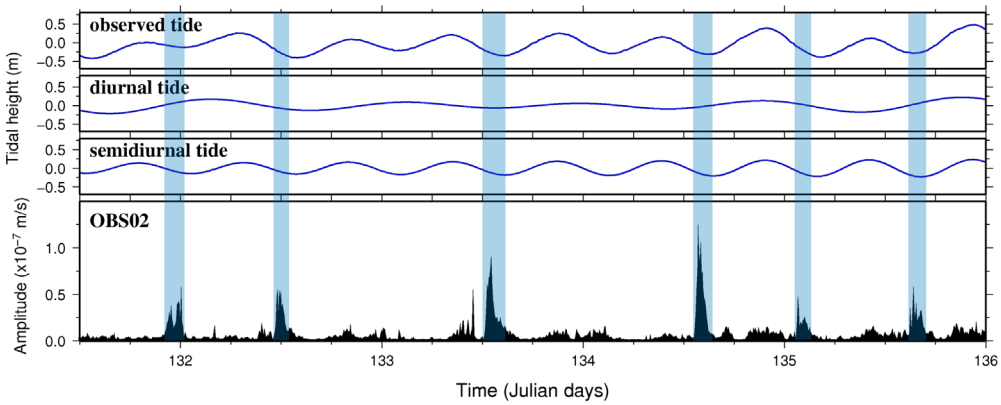

Fig. 9. Close-ups of the tremor activities at OBS02 site, compared to the observed tides, diurnal and semidiurnal constituents, respectively, from May 12 to May 16, 2011. The light blue areas mark the long-duration tremors occurring around lower low tides, but no obvious long-duration tremors at the rising periods to the higher high tides. (For interpretation of the references to color in this figure legend, the reader is referred to the web version of this article.)

only happen when the pore-fluid pressure in sediments reaches the vertical stress of the overlying sediments. Thus, in most of the insufficient gas charge contexts, the gas (fluid) expulsions may favor the occurrence at low tides. Most gas emissions at low tides for the Hydrate Ridge in the Cascadia margin (Torres et al., 2002) or for the near-shore area of Santa Barbara, California (Boles et al., 2001) may be attributed to such a situation.

Ocean tides only contribute slight stress variation on the seabed. A large storm or dramatic change of sea level can significantly change stress conditions of the seabed, which is thus expected to more likely induce methane emissions and tremors in a gas-rich seabed. Methane is known as the most significant component of greenhouse gases. In this scenario, a massive emission of methane from the seafloor has a strong impact on Earth climate change. On the other hand, persistently gas emissions and long-duration tremors could gradually weaken the strength of a gassy seabed of a continental slope, which enhance potential of slope failures causing submarine landslides and turbidity currents. Strong turbidity currents can heavily jeopardize underwater constructions, such as breakages of submarine telecommunication cables (Heeze and Ewing, 1952; Hsu et al., 2008). It is suggested that when sea levels are lower during glacial periods, more dissociated methane would be released from continental slopes and the seabed would be less stable (Nisbet and Piper, 1998; Rothwell et al., 1998).

5. Conclusions

The incipient orogeny off SW Taiwan has created folds and thrusts and has being uplifted seafloor; gas hydrate then becomes unstable and may disassociate at the water depth of ~650 m. In consequence, gases such as methane and carbon dioxide discharge out of the seabed and mud diapirs, mud volcanoes and pockmarks are widely distributed off SW Taiwan. By observing 38 kHz acoustic images of seawater column above active mud volcano MV1, we find that the gas emissions display a temporal variation. The gas emissions out of the seabed may occur in either a quiet way or in an eruptive way. The latter simultaneously induce tremors of the seabed.

By examining the seismic records of our deployed OBSs around MV1, we find that the gas emissions and associated tremors are closely modulated by the ocean tide. Strong gas emissions and long-duration tremors usually occur during both the rising periods to the higher high tides and the falling periods to the lower low tides. The former case is mainly controlled by the diurnal constituents, while the latter case is mainly controlled by the semidiurnal constituents. For the gas expulsions out of the seabed occurring at the rising tides, the pore-fluid pressure due to the gas charging from a deeper source to the shallow sediments must be sufficient to overcome the vertical stress from the overlying sediments and seawater at high tides. The sufficient gas in the shallow sediments may also provide enough pore-fluid pressure to overcome the vertical stress from the overlying sediments and seawater at low tides. However, in the case of few or poor gas charging to shallow sediments, gas expulsions and tremors preferably occur at lower low tides, because the vertical stress from the overlying sediments and seawater is lowest at lower low tides. In any case, during a tidal day the average of the tremor amplitudes (and the gas emission intensity) is positively proportional to the tidal range. For most of the time, the seafloor off SW Taiwan oscillates around 7 Hz because of gas expulsions.

Acknowledgments

Discussions and comments from H. Kao, P.-F. Chen, K.-F. Ma, T.A. Lin, C.-C. Chen and L. Armada are appreciated. S.-D. Chiu, C.-W. Liang, C.-H. Tsai, and Y.-F. Ma are acknowledged for their help in data acquisition. W.-B. Doo, T.S. Kuo and S.-S. Lin helped prepare some figures. This work is supported by National Science Council, Taiwan and partly by the gas-hydrate program of Central Geological Survey, Taiwan.

References

Boles, J.R., Clark, J.F., Leifer, I., Washburn, L., 2001. Temporal variation in natural methane seep rate due to tides, Coal Oil Point area, California. J. Geophys. Res. 106, 27077–27086.
Chen, S.-C., Hsu, S.-K., Tsai, C.-H., Ku, C.-Y., Yeh, Y.-C., Wang, Y., 2010. Gas seepage, pockmarks and mud volcanoes in the near shore of SW Taiwan. Mar. Geophys. Res. 31, 133–147.
Chi, W.-C., Reed, D.L., Tsai, C.-C., 2006. Gas hydrate stability zone offshore southern Taiwan. Terr. Atmos. Oceanic Sci. 17, 829–843.
Chiu, J.-K, Tseng, W.-H, Liu, C.-S., 2006. Distribution of gassy sediments and mud volcanoes offshore southwestern Taiwan. Terr. Atmos. Oceanic Sci. 17, 703–722.
Chuang, P.-C., Yang, T.F., Hong, W.-L., Lin, S., Sun, C.-H., Lin, A.T., Chen, J.-C., Wang, Y., Chung, S.-H., 2010. Estimation of methane flux offshore SW Taiwan and the influence of tectonics on gas hydrate accumulation. Geofluids 10, 497–510.
Chuang, P.-C., Yang, T.F., Lin, S., Lee, H.-F., Lan, T.F., Hong, W.-L., Liu, C.-S., Chen, J.-C., Wang, Y., 2006. Extremely high methane concentration in bottom water and cored sediments from offshore southwestern Taiwan. Terr. Atmos. Oceanic Sci. 17 (4), 903–920.
Custodio, S.I.S., Fonseca, J.F.B.D., d'Oreye, N.F., Faria, B.V.E., Bandomo, Z., 2003. Tidal modulation of seismic noise and volcanic tremor. Geophys. Res. Lett. 30 (15), 1816, http://dx.doi.org/10.1029/2003GL016991.
Dimitrov, L.I., 2003. Mud volcanoes—the most important pathway for degassing deeply buried sediments. Geo-Mar. Lett. 23, 155–161.
Etiope, G., Klusman, R., 2002. Geologic emissions of methane to the atmosphere. Chemosphere 49, 777–789.
Heeze, B.C., Ewing, M., 1952. Turbidity currents and submarine slumps, and the 1929 Grand Banks earthquake. Am. J. Sci. 250, 849–873.

Hsu, S.-K., Kuo, J., Lo, C.-L., Tsai, C.-H., Doo, W.B., Ku, C.-Y., Sibuet, J.-C., 2008. Turbidity currents, submarine landslides and the 2006 Pingtung earthquake off SW Taiwan. Terr. Atmos. Oceanic Sci. 19, 767–772.
Hu, C.-K., Chiu, C.-T., Chen, S.-H., Kuo, J.-Y., Jan, S., Tseng, Y.-H., 2010. Numerical simulation of barotropic tides around Taiwan. Terr. Atmos. Oceanic Sci. 21, 71–84.
Judd, A., Hovland, M., 2007. Seabed Fluid Flow. University Press, Cambridge, United Kingdom, pp. 475.
Judd, A.G., 2003. The global importance and context of methane escape from the seabed. Geo-Mar. Lett. 23, 147–154.
Kasahara, J., 2002. Tides, earthquakes, and volcanoes. Science 297, 348–349.
Kopf, A.J., 2002. Significance of mud volcanism. Rev. Geophys. 40 10.1029/2000RG000093.
Lambert, A., Kao, H., Rogers, G., Courtier, N., 2009. Correlation of tremor activity with tidal stress in the northern Cascadia subduction zone. J. Geophys. Res. 114 10.1029/2008JB006038.
Lim, Y.-C., Lin, S., Yang, T.F., Chen, Y.-G., Liu, C.-S., 2011. Variations of methane induced pyrite formation in the accretionary wedge sediments offshore southwestern Taiwan. Mar. Petrol. Geol. 28, 1829–1837.
Liu, C.-S., Schnurle, P., Wang, Y.-S., Chung, S.-H., Chen, S.-C., Hsiuan, T.-H., 2006. Distribution and characters of gas hydrate offshore of southwestern Taiwan. Terr. Atmos. Oceanic Sci. 17, 615–644.
Lo, C.-L., Hsu, S.-K., 2005. Earthquake-induced gravitational potential energy change in the active Taiwan orogenic belt. Geophys. J. Int. 162, 169–172.
Nakata, R., Suda, N., Tsuruoka, H., 2008. Non-volcanic tremor resulting from the combined effect of Earth tides and slow slip events. Nat. Geosci. 1, 676–678.
Nisbet, E.G., Piper, D.J.W., 1998. Giant submarine landslides. Nature 392, 329.
Rothwell, R.G., Thomson, J., Kähler, G., 1998. Low-sea-level emplacement of a very large Late Pleistocene 'megaturbidite' in the western Mediterranean Sea. Nature 392, 377–380.
Rubinstein, J.L., Rocca, M.L., Vidal, J.E., Creager, K.C., Wech, A.G., 2008. Tidal Modulation of Nonvolcanic Tremor. Science 319, 186–189.
Shelly, D.R., Beroza, G.C., Ide, S., Nakamula, S., 2006. Low-frequency earthquakes in Shikoku, Japan, and their relationship to episodic tremor and slip. Nature 442, 188–191.
Shelly, D.R., Beroza, G.C., Ide, S., 2007. Complex evolution of transient slip derived from precise tremor locations in western Shikoku, Japan. Geochem. Geophys. Geosyst. 8, Q10014.
Sibuet, J.-C., Hsu, S.-K., 2004. How was Taiwan created? Tectonophysics 379, 159–181.
Sloan, E.D., 1998. Gas Hydrates: relevance to world margin stability and climate change. In: Henriet, J.P, Mienert, J. (Eds.), Geological Society. Special Publications, London.
Thomas, A.M., Nadeau, R.M., Bürgmann, R., 2009. Tremor–tide correlations and near-lithostatic pore pressure on the deep San Andreas Fault. Nature 462, 1048–1051.
Tolstoy, M., Vernon, F.L., Orcutt, J.A., Wyatt, F.K., 2002. Breathing of the seafloor: tidal correlations of seismicity at Axial volcano. Geology 30, 503–506.
Torres, M.E., McManus, J., Hammond, D.E., de Angelis, M.A., Heeschen, K.U., Colbert, S.L., Tryon, M.D., Brown, K.M., Suess, E., 2002. Fluid and chemical fluxes in and out of sediments hosting methane hydrate deposits on Hydrate Ridge, OR, I: Hydrological provinces. Earth Planet. Sci. Lett. 201, 525–540.
Yang, T.F., Chuang, P.-C., Lin, S., Chen, J.-C., Wang, Y., Chung, S.-H., 2006. Methane venting in gas hydrate potential area offshore of SW Taiwan: evidence of gas analysis of water column samples. Terr. Atmos. Oceanic Sci. 17 (4), 933–950.
Yang, T.F., Yeh, G.-H., Fu, C.-C., Wang, C.-C., Lan, T.F., Lee, H.-F., Chen, C-H., Walia, V., Sung, Q.-C., 2004. Composition and exhalation flux of gases from mud volcanoes in Taiwan. Environ. Geol. 46, 1003–1011.
You, C.-F, Gieskes, J.-M, Lee, T., Yui, T.-F, Chen, H.-W., 2004. Geochemistry of mud volcano fluids in the Taiwan accretionary prism. Appl. Geochem. 19, 695–707.